His[68] and His[141] Are Critical Contributors to the Intersubunit Catalytic Site of Adenylosuccinate Lyase of *Bacillus subtilis*[†]

Tom T. Lee,[‡] Carolyn Worby,[§] Zhao-Qin Bao,[§] Jack E. Dixon,[§] and Roberta F. Colman*,[‡]

Department of Chemistry and Biochemistry, University of Delaware, Newark, Delaware 19716, and Department of Biological Chemistry, University of Michigan Medical School, Ann Arbor, Michigan 48109

Received September 24, 1998

ABSTRACT: Mutant adenylosuccinate lyases of *Bacillus subtilis* were prepared by site-directed mutagenesis with replacements for His[141], previously identified by affinity labeling as being in the active site [Lee, T. T., Worby, C., Dixon, J. E., and Colman, R. F. (1997) *J. Biol. Chem. 272*, 458−465]. Four substitutions (A, L, E, Q) yield mutant enzyme with no detectable catalytic activity, while the H141R mutant is about 10^{-5} as active as the wild-type enzyme. Kinetic studies show, for the H141R enzyme, a K_m that is only 3 times that of the wild-type enzyme. Minimal activity was also observed for mutant enzymes with replacements for His[68] [Lee, T. T., Worby, C., Bao, Z.-Q., Dixon, J. E., and Colman, R. F. (1998) *Biochemistry 37*, 8481−8489]. Measurement of the reversible binding of radioactive adenylosuccinate by inactive mutant enzymes with substitutions at either position 68 or 141 shows that their affinities for substrate are decreased by only 10−40-fold. These results suggest that His[141], like His[68], plays an important role in catalysis, but not in substrate binding. Evidence is consistent with the hypothesis that His[141] and His[68] function, respectively, as the catalytic base and acid. Circular dichroism spectroscopy and gel filtration chromatography conducted on wild-type and all His[141] and His[68] mutants reveal that none of the mutant enzymes exhibits major structural changes and that all the enzymes are tetramers. Mixing inactive His[141] with inactive His[68] mutant enzymes leads to striking increases in catalytic activity. This complementation of mutant enzymes indicates that His[141] and His[68] come from different subunits to form the active site. A tetrameric structure of adenylosuccinate lyase was constructed by homology modeling based on the known structures in the fumarase superfamily, including argininosuccinate lyase, δ-crystallin, fumarase, and aspartase. The model suggests that each active site is constituted by residues from three subunits, and that His[141] and His[68] come from two different subunits.

Adenylosuccinate lyase (EC 4.3.2.2) catalyzes two distinct reactions in purine biosynthesis: the conversions of 5-amino-4-imidazole-*N*-succinocarboxamide ribotide to 5-amino-4-imidazolecarboxamide ribotide and fumarate, and the cleavage of adenylosuccinate to form AMP and fumarate (*1*). The deficiency of adenylosuccinate lyase in humans has been known since 1984 (*2*−*4*). The principal symptom of the deficiency is psychomotor retardation, in which the patients exhibit elevated levels of two normally undetectable compounds, succinylaminoimidazole carboxamide riboside and succinyladenosine. Point mutations that have been discovered in genes associated with defective enzyme include P75A/D397Y (*5*), R401H (*6*), and S413P (*7*). In the case of S413P, the mutation apparently generates a structural change in the protein leading to an unstable but catalytically competent enzyme.

The steady-state kinetics and inhibition studies suggest a uni−bi mechanism with a strongly preferred sequence of product release, in which fumarate leaves the enzyme before AMP (*7*−*10*). It has been proposed that the cleavage reaction proceeds by a β-elimination mechanism, which involves the attack of an enzymic general base on the β-H, and that elimination of the N-6 amino group is facilitated by protonation of the N-1 ring nitrogen or amide oxygen by an amino acid of the enzyme functioning as a general acid (*11*).

The sequence of *Bacillus subtilis* adenylosuccinate lyase shows 26% identity plus 17% similarity to the human enzyme. Previously, we have implicated His[68] and His[141] in the active site of *B. subtilis* enzyme by affinity labeling with 6-(4-bromo-2,3-dioxobutyl)thioadenosine 5′-monophosphate (*12*) and 2-[(4-bromo-2,3-dioxobutyl)thio]adenosine 5′-monophosphate (*13*). The role of His[68] as a key catalytic residue has been evaluated by site-directed mutagenesis (*13*). Here, we describe the characterization of His[141] mutants.

Intersubunit complementation is a phenomenon which can be observed in a multisubunit protein if the active site is located between two or more subunits. In complementation experiments, active sites are generated from inactive mutant subunits with substitutions for different amino acids; these hybrid enzymes can be prepared either by coexpression of the mutant genes or by dissociation of individual mutant multimers followed by reassociation to form mixed mutant multimers. Complementation can occur when the mutated

[†] This work was supported by National Science Foundation Grant MCB-97-28202 (to R.F.C.) and United States Public Health Service Grant RO1 DK 18849 (to J.E.D.).

* To whom correspondence should be addressed. Phone: 302-831-2973. Fax: 302-831-6335. E-mail: rfcolman@udel.edu.

[‡] University of Delaware.

[§] University of Michigan Medical School.

10.1021/bi982299s CCC: $18.00
Published on Web 12/08/1998

active-site amino acids come from different subunits of the enzyme (*14*−*17*). In this paper, we report the reactivation of mixtures of His^{68}/His^{141} mutant enzymes. The recovery of activity shows that the active site of adenylosuccinate lyase includes amino acids contributed by two or more subunits.

Adenylosuccinate lyase belongs to the fumarase superfamily, a group of functionally related enzymes which act on different substrates to generate fumarate as one of the products. The family includes class II fumarase (EC 4.2.1.2), aspartase (EC 4.3.1.1), argininosuccinate lyase (EC 4.3.2.1), δ-crystallin, and adenylosuccinate lyase. Despite the low sequence homology within the family, crystal structures determined for members of the family exhibit considerable similarity. In this paper, we present a structure of adenylosuccinate lyase constructed by homology modeling and propose roles for active site amino acid residues important for catalysis.

EXPERIMENTAL PROCEDURES

Materials. Adenylosuccinate, adenosine 5′-monophosphate, fumarate, MES,[1] and HEPES were purchased from Sigma. [2-^{3}H]Adenosine 5′-monophosphate was supplied by Amersham Life Science. The protein assay concentrate was from Bio-Rad. All other chemicals were of reagent grade.

Site-Directed Mutagenesis. Site-directed mutagenesis of pBHis was performed using the QuikChange site-directed mutagenesis kit (Stratagene, La Jolla, CA). The oligonucleotides used for Arg^{67} and His^{68} were described previously (*13*). The oligonucleotides used for His^{141} were CGC ACA GCC GGC GTA (H141A), CGC ACA CTC GGC GTA (H141L), CGC ACA GAG GGC GTA (H141E), GGG CGC ACA CAG GGC GTA CAC (H141Q), CGC ACA CGC GGC GTA (H141R), and their complements. All mutations were confirmed by nucleotide sequence analysis.

The plasmid was expressed in *E. coli* strain BL21 (DE3) and the mutant enzymes were purified to homogeneity as described previously (*12*, *18*). The purity of the mutant proteins was assessed by 12% SDS−polyacrylamide gel electrophoresis and the N-terminal amino acid sequences were checked by gas-phase sequencing.

Kinetics of B. subtilis Adenylosuccinate Lyase. The activity of the wild-type and mutant adenylosuccinate lyase was measured from the decrease in absorbance at 282 nm using the difference extinction coefficient of 10 000 M^{-1} cm^{-1} between adenylosuccinate and AMP, as described earlier (*12*). An adenylosuccinate concentration of 60 μM was used to determine the specific activity. The enzyme was preincubated in 20 mM potassium phosphate (pH 7.0) containing 20 mM NaCl at 25 °C for 30 min before activity measurements were made.

Circular Dichroism of the Wild-Type and Mutant Enzymes. Circular dichroism was conducted using a Jasco model J-710 spectropolarimeter. Measurements of the ellipticity as a function of wavelength at 0.1 nm increments between 250 and 200 nm were made using a 0.1 cm path length cylindrical quartz cell. Purified recombinant protein samples (0.1−0.2 mg/mL) in 20 mM potassium phosphate (pH 7.0) containing 20 mM NaCl were preincubated at 25 °C for 30 min before CD measurements. Each scan was repeated 5 times and averaged. The background from the buffer was subtracted from all spectra. Protein concentration assays were used to determine the exact amount of protein in each sample. The mean residue molar ellipticity $[\theta]$ (deg cm^2 $dmol^{-1}$) was calculated from the equation $[\theta] = \theta/(100nCl)$, where θ is the measured ellipticity in millidegrees, C is the molar concentration of protein in molarity, l is the path length of cell in centimeters, and n is the number of residues per subunit of adenylosuccinate lyase (437 including the His_6 tag).

FPLC of the Wild-Type and Mutant Enzymes. Gel filtration was conducted using a Pharmacia FPLC system equipped with a Superose-12 column (1 × 30 cm Pharmacia) equilibrated with 20 mM potassium phosphate (pH 7.0) containing 20 mM NaCl. For each analysis, 0.2 mL of 0.2−1.5 mg/mL purified protein was applied to the column at a flow rate of 0.3 mL/min. Molecular weight calibration kits (Pharmacia) were used to generate a standard curve.

Determination of Equilibrium Constant. Adenylosuccinate lyase catalyzes the reversible cleavage of adenylosuccinate. The equilibrium constant was determined spectrophotometrically by measuring the absorbance difference before and after the reaction reached equilibrium. Tandem quartz cuvettes with a total path length of 1 cm (equally divided) were used. One milliliter of 0.2 mg/mL wild-type adenylosuccinate lyase and 1 mL of 100 μM adenylosuccinate plus 2−16 mM fumarate (pH 7.0) were placed in separate compartments of the cuvette. Both solutions were buffered in 50 mM HEPES (pH 7.0). The absorbance at 290 nm (A_0) was recorded before completely mixing the two compartments. The reaction was carried out at 25 °C and reached equilibrium in 20 min as judged by the constant absorbance at 290 nm (A_{eq}). This wavelength allowed us to include higher fumarate concentrations than is possible at 282 nm. The change in absorbance (ΔA) was calculated by ($A_0 - A_{eq}$). Since the fumarate concentration is in excess, the equilibrium constant (K_{eq}) can be expressed as

$$K_{eq} = \frac{[\mathrm{AMP}]_{eq}[\mathrm{Fumarate}]_{eq}}{[\mathrm{Adenylosuccinate}]_{eq}} = \frac{(\Delta A/\Delta\epsilon)[\mathrm{F}]_0}{[\mathrm{S}]_0 - (\Delta A/\Delta\epsilon)} \quad (1)$$

where $\Delta\epsilon$ is the difference extinction coefficient at 290 nm between adenylosuccinate and AMP (3800 M^{-1} cm^{-1}), $[F]_0$ the initial fumarate concentration, and $[S]_0$ the initial adenylosuccinate concentration. Rearrangement of eq 1 generates

$$[\mathrm{F}]_0 = (K_{eq}\Delta\epsilon[\mathrm{S}]_0)(1/\Delta A) - K_{eq} \quad (2)$$

K_{eq} can be obtained from the y-intercept of the linear plot of $[F]_0$ against $(1/\Delta A)$. Figure 1 shows that, at a fixed concentration of adenylosuccinate, the change in absorbance is linear with the initial concentration of fumarate. The equilibrium constant as determined starting with adenylosuccinate was 0.0069 M from the y-intercept of $[F]_0$ against $(1/\Delta A)$.

Preparation of [2-^{3}H]Adenylosuccinate. [2-^{3}H]Adenylosuccinate was synthesized enzymatically from [2-^{3}H]AMP. The reaction was carried out in 25 mM HEPES (pH 7.0)

[1] Abbreviations: MES, 2-(*N*-morpholino)ethanesulfonic acid; HEPES, *N*-(2-hydroxyethyl)piperazine-*N*′-2-ethane sulfonic acid; HPLC, high-performance liquid chromatography; CD, circular dichroism; ASL, adenylosuccinate lyase; SCR, structurally conserved region; PDF, probability density function.

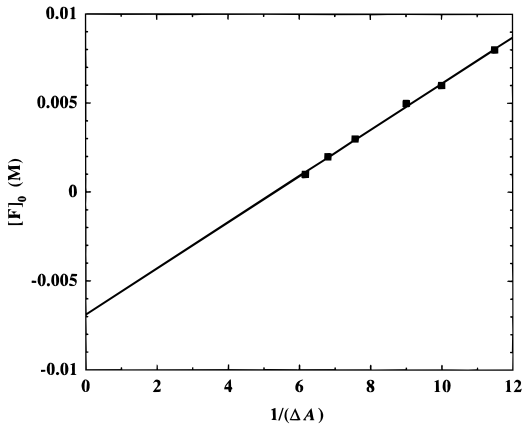

FIGURE 1: Determination of the equilibrium constant of the cleavage reaction. The initial concentration of fumarate was plotted against the change in absorbance after equilibrium. The measurement was performed using tandem quartz cuvettes as described in Experimental Procedures.

containing 10 mM [2-^{3}H]AMP (2 μCi), 200 mM fumarate, and 0.05 mg/mL *B. subtilis* adenylosuccinate lyase. The enzyme was removed by centrifugation of the reaction at 5000 rpm using Centricon-10 (Amicon) after 1 h of incubation at 25 °C. The filtrate was applied to a DE-52 column (1 × 23 cm) preequilibrated with 10 mM ammonium acetate (pH 6.8), and the AMP, adenylosuccinate, and fumarate were separated by a linear gradient from 10 mM ammonium acetate (pH 6.8, 1 L) to 500 mM ammonium acetate (pH 6.8, 1 L). Fractions of 12 mL were collected, and the spectra and radioactivity were measured. The adenylosuccinate was eluted much later (~250 mM ammonium acetate) than the other two compounds. The fractions containing [2-^{3}H]-adenylosuccinate were pooled and lyophilized thoroughly to remove the salt. The pure [2-^{3}H]adenylosuccinate was dissolved in water and had a specific radioactivity of 1.3 × 10^{11} cpm/mol. The overall yield was 60%.

Measurement of Adenylosuccinate Binding by Enzymes. The dissociation constant of adenylosuccinate for the wild-type adenylosuccinate lyase was determined kinetically by measuring its K_I as a competitive inhibitor with respect to AMP. The K_m for AMP in the back reaction was measured in the presence of 10 mM fumarate and in the absence and presence of 2.5 and 5 μM adenylosuccinate at 290 nm. The dissociation constants of adenylosuccinate for the inactive mutant enzymes were determined by ultrafiltration. To a Centricon-10 membrane system (Amicon, pretreated with 50 mM HEPES to remove the glycerol coating) was added 40 μL of mutant adenylosuccinate lyase (20−50 mg/mL), 200 μL of [2-^{3}H]adenylosuccinate, and 560 μL of 50 mM HEPES (pH 7.0). The final concentration of [2-^{3}H]adenylosuccinate was varied from 20 to 500 μM. The exact total concentration of [2-^{3}H]adenylosuccinate was determined by measuring the radioactivity of aliquots using a Packard Tri-Carb liquid scintillation analyzer (model 1500). Centrifugation was then carried out at 5000 rpm and 25 °C for 5 min. The initial filtrate (~200 μL) was discarded before the second centrifugation run under the same conditions. Control samples without the enzyme were analyzed in parallel to determine the recovery after the ultrafiltration. This value, usually around 90%, was used as a correction factor to calculate the free adenylosuccinate concentration from the second filtrate. The concentration of bound adenylosuccinate was calculated by subtraction of the free from the total concentration.

pH Dependence of the Reaction Catalyzed by Adenylosuccinate Lyase. pH profiles for the reaction catalyzed by the mutant and wild-type enzyme were determined over the range of pH 6−9. The buffers contained 50 mM MES and 50 mM HEPES. The ionic strength of each buffer was adjusted to 0.1 M with NaCl. The reaction rate was measured using 100 μM adenylosuccinate as substrate.

Reactivation of Activities of Mutant Enzymes. Various mixtures of His^{68} and His^{141} mutant enzymes (both at 0.7 mg/mL) in 20 mM potassium phosphate containing 20 mM NaCl (pH 7.0) were incubated at 25 °C. The reactivation of enzymatic activity was monitored as a function of time. For control experiments, 1.4 mg/mL wild-type enzyme and a combination of 0.7 mg/mL wild type and mutant enzymes were incubated as well. The K_m values of the hybrid enzymes were determined after 10 h incubation.

Molecular Modeling of B. subtilis Adenylosuccinate Lyase. Since the crystal structure of adenylosuccinate lyase has not yet been solved (*18*), modeling studies were carried out on an SGI workstation using the *Insight II* molecular modeling system (Biosym/MSI, San Diego, CA). Four proteins were used as reference structures: *E. coli* fumarase C, *E. coli* aspartase, human argininosuccinate lyase and duck δ2-crystallin. Their SWISS-PROT ID codes, accession numbers, and PDB ID codes are FUMC_ECOLI, P76891, 1FUO (*19*); ASPA_ECOLI, P78140, 1JSW (*20*); ARLY_HUMAN, P04424, 1AOS (*14*); and CRD2_ANAPL, P24058, 1AUW (*21*), respectively.

The initial attempt to structurally align the four reference proteins using the automatic alignment program employed by Homology module did not generate any useful information. The overall homology among them appears to be too low for the program to identify the structurally conserved regions (SCRs). Therefore, structural alignment was performed by manually comparing backbone atoms in the peptide segments in Homology. Preferred alignments were decided by monitoring RMS deviation values. Alternatively, sequence alignment was performed pairwise using Ψ-BLAST search (*22*) and SIM local similarity program (*23*). Both programs report sequence alignment of the longest fragment with significant similarity. This fragment encompasses the entire domain **II** and, in most cases, various lengths of domain **I** and **III**. SIM also reports alignments of small high-scoring fragments, which were used to align the rest of the sequences. Final alignment was achieved by optimizing both structural and sequence alignment. Results from pairwise alignment were then integrated to generate the multiple alignment by aligning the SCRs.

The next step was the alignment of the sequence of *B. subtilis* adenylosuccinate lyase with the reference proteins. This was obtained initially by a combination of Ψ-BLAST and SIM. For the regions whose alignments were not well defined, adjustments were made to generate alternate alignments for later stages.

The modeling was performed using the Modeler program under the Homology. This is an automated homology modeling program that calculates an all-atom model using combined information from the sequence alignment and the structures of reference proteins. Spatial restraints, expressed as probability density functions (PDFs) from the reference

proteins, are optimized to obtain the model. The model with the lowest value of objective function (*F*, molecular PDF violation) fits best to the reference structures. In the search for the best alignment, three models were generated from each different initial alignment using the Medium optimization protocol (fast molecular dynamics simulated annealing). The best alignment was selected by comparing the lowest *F* values. To simplify the procedure, the three domains were analyzed separately. The final alignment was obtained by the combination of the best alignment for each domain.

Since the number of residues in the tetramer of adenylosuccinate lyase (1724) is too large for the current version of Modeler, we took an alternative route to solve the problem. Five models for a monomer were generated using the High optimization protocol (thorough molecular dynamics simulated annealing). The best model (with lowest *F*) was selected as the temporary structure for all four protomers. This was based on the high structural similarity among the protomers in reference proteins. The tetramer was built by assembling four identical protomer models. Superimposition of each protomer with the corresponding protomer of reference proteins generated an initial structure of the tetramer, which was then subjected to *Discover 3.00* to calculate the energy-minimized structure using the steepest descent and conjugate gradient methods.

The structure of adenylosuccinate was constructed using Builder module. The most extended form after energy minimization was docked into the active-site pocket. The β-carboxylate of the substrate was guided to the vicinity of the side chains of Lys^{268} and Asn^{270}. This choice was based on the fumarase-inhibitor complex structures which exhibit conserved positions for the corresponding carboxylate (*19, 24, 25*). The arrangement of the substrate was adjusted to minimize the energy by van der Waals and electrostatic interactions. The complex was then subjected to *Discover 3.00* for extensive energy minimization.

RESULTS

Kinetic Parameters of the Wild-Type and Mutant Enzymes with Substitutions for His^{141}. Affinity-labeling experiments published previously (*12*) indicated that 6-(4-bromo-2,3-dioxobutyl)thioadenosine 5′-monophosphate modified His^{141} of *B. subtilis* adenylosuccinate lyase. To evaluate the results of our previous affinity-labeling experiments, site-directed mutagenesis was used to construct enzymes with substitutions for His^{141}. The mutant enzymes were constructed, expressed, purified and their purity ascertained. Similar approaches were used to generate mutations at His^{68} (*13*). The kinetic parameters of these mutants are summarized in Table 1. The specific activity was measured under standard assay conditions using 60 μM adenylosuccinate and pH 7.0 buffer at 25 °C. All five mutants exhibit a striking decrease in specific activity. The decreases of more than 10000-fold strongly suggest an important role for His^{141} in enzyme function, consistent with our affinity-labeling results (*12*). In fact, as Table 1 shows, four of the five mutants do not have detectable activities. Only the H141R mutant has measurable activity; the k_{cat} and K_m of this mutant are also shown in Table 1. The 60000-fold decrease in k_{cat} for H141R is significantly larger than the 3-fold increase in K_m, indicating that mutation causes a more dramatic effect on catalysis than on substrate binding.

Table 1: Comparison of the Kinetic Parameters of the Wild-Type and His^{141} Mutants of Adenylosuccinate Lyase[a]

	specific activity (μmol/min/mg)	k_{cat} (s^{-1})	K_m (μM)	k_{cat}/K_m (M^{-1} s^{-1})
wild-type	2.0	1.7 ± 0.1	2.6 ± 0.4	6.5×10^5
H141A	0[b]	*c*	*c*	*c*
H141L	0[b]	*c*	*c*	*c*
H141E	0[b]	*c*	*c*	*c*
H141Q	0[b]	*c*	*c*	*c*
H141R	3.0×10^{-5}	$(2.8 \pm 0.1) \times 10^{-5}$	6.7 ± 1.1	4.2

[a] The specific activities were measured under standard assay conditions, as described in the Experimental Procedures. The k_{cat} and K_m constants were determined by varying the concentration of adenylosuccinate and fitting the data to the Michaelis−Menten equation. [b] The specific activities of these four mutants were below the detection limit which was $(1.3-4.9) \times 10^{-5}$ μmol/min/mg depending on the protein concentration of the expressed mutant enzyme. [c] Not determined.

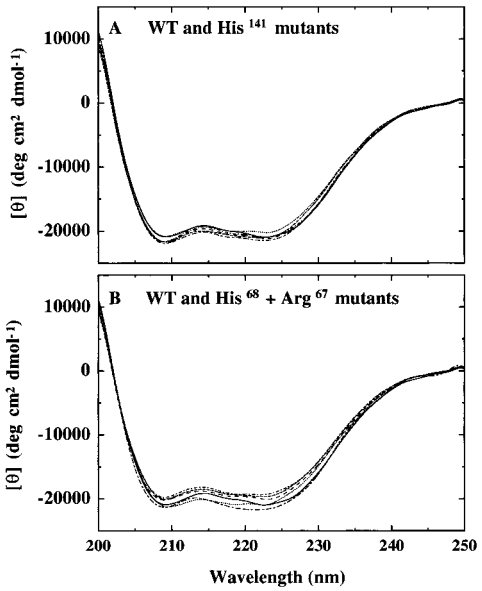

FIGURE 2: Far-UV CD spectra of the wild-type and mutant enzymes. (A) Wild-type (—), H141A (•••), H141L (- - -), H141E (-•-•-), H141Q (— — —), and H141R (—•—•—). (B) Wild-type (—), H68A (•••), H68K (- - -), H68Q (-•-•-), R67M (—•—•—), and R67M: H68Q (— — —). Each spectrum shown represents the average of five scans. Minima occur at 208 and 223 nm.

Circular Dichroism Spectra of the Wild-Type and All Mutant Enzymes. CD spectra were measured to provide some information on the secondary structure as well as to ascertain whether any conformational changes were caused by the mutations at positions 141 or 68. As shown in Figure 2, the spectra of all mutants were, within the experimental error, essentially superimposable on that of the wild-type enzyme. These results exclude the possibility that the loss of activity in the mutant enzymes is due to large conformational change: none of the mutations has a major impact on the secondary structure of the enzyme, as indicated by circular dichroism.

The percentage of α-helix in the active form of the enzyme can be estimated from the equation

$$\% \ \alpha\text{-helix} = \frac{[\theta]_{208nm} - 4000}{33000 - 4000} \times 100 \qquad (3)$$

where $[\theta]_{208nm}$ is the mean residue molar ellipticity at 208 nm. The data were analyzed using GraphPad software InPlot

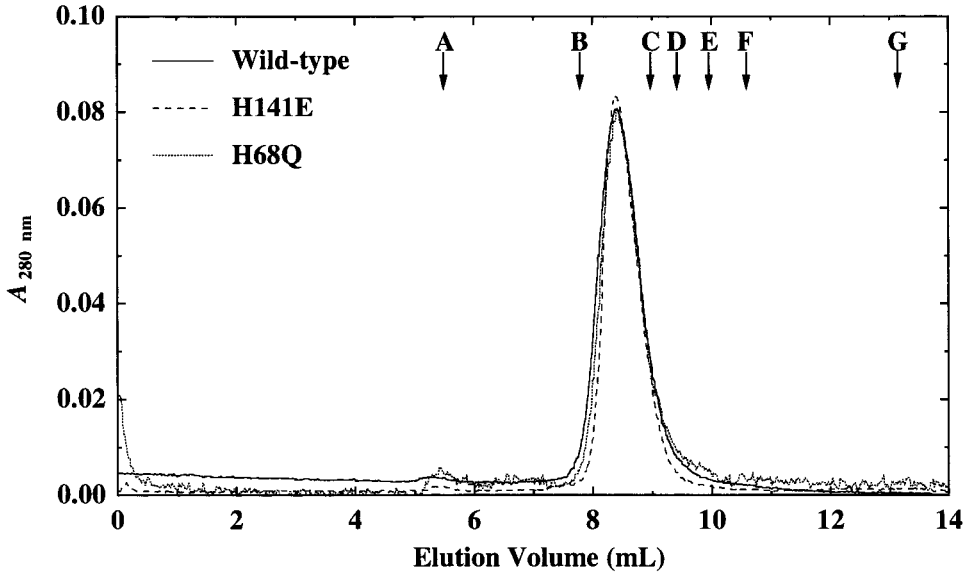

FIGURE 3: Superose-12 FPLC elution profile of the wild-type and mutant adenylosuccinate lyases. The enzymes (preincubated for 30 min) were applied to a Superose-12 column equilibrated with 20 mM potassium phosphate (pH 7.0) containing 20 mM NaCl. The column was calibrated with molecules of known MW including ferritin (B, 440 kDa), catalase (C, 232 kDa), aldolase (D, 158 kDa), albumin (E, 67 kDa), ovalbumin (F, 43 kDa), and chymotrypsinogen A (G, 25 kDa). The elution positions of the standard proteins are indicated on top. The column has a total volume (V_t) of 24 mL and a void volume (V_o) of 5.7 mL, as determined by Blue Dextran 2000 (A).

for least-squares parameter evaluation. The adenylosuccinate lyase was estimated to have an α-helical content of about 50−60%. The percentage of α-helix and sheet for the solved structures in the superfamily (1FUO, 1JSW, 1AOS, and 1AUW) are 54−62 and 4−7%, respectively. Thus, our results are consistent with the superfamily having similar secondary structure.

Gel Filtration FPLC of the Wild-Type and Mutant Enzymes. The active form of adenylosuccinate lyase from various sources is tetrameric. To verify the *B. subtilis* enzyme as a tetramer, as well as to evaluate whether or not the oligomeric state of the enzyme is influenced by any of these mutations, gel filtration under native conditions was conducted using a Superose-12 FPLC column (Figure 3). $(V_e - V_o)/(V_t - V_o)$ was plotted against $\log(M_r)$ to generate the standard curve (not shown), based on which the apparent molecular mass of *B. subtilis* adenylosuccinate lyase (V_e = 8.4 mL) was estimated to be 245 kDa. Adenylosuccinate lyase elutes between proteins B (ferritin) and C (catalase), consistent with a protein of about 245 kDa, or the tetrameric form of the enzyme. No absorbance was observed in regions of dimer and monomer elution.

The same experiments were carried out on all the mutants including H141A, H141L, H141E, H141Q, H141R, H68A, H68K, H68Q, R67M, and R67M:H68Q. For simplicity, only H141E and H68Q are shown in Figure 3. All mutant enzymes were eluted at the same position as the wild-type. Moreover, every peak had a half-peak width of 0.8 mL, indicating that the subunits were associated. These results suggest that the mutations do not affect the oligomeric state of the enzyme.

Binding of Adenylosuccinate to the Mutant Enzymes. Except for the H141R mutant, all substitutions for His^{141} decreased the activity to an undetectable level (Table 1). Likewise, H68A and H68K are also inactive, as previously described (*13*). The kinetic parameters for these mutants cannot be determined from a standard enzymatic assay. However, it is important to know whether these mutant enzymes retain the ability to bind the substrate. Therefore,

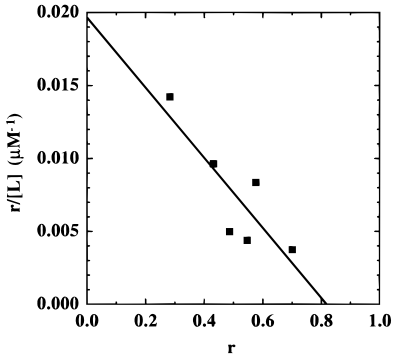

FIGURE 4: Plot of *r*/[L] against *r* for H141E mutant. The concentrations of adenylosuccinate in free and bound form were measured as described in Experimental Procedures. The dissociation constants were determined from (−1/slope).

the dissociation constants were measured by ultrafiltration using enzymatically synthesized [2-^{3}H]adenylosuccinate as the substrate. Enzyme samples in solutions containing various substrate concentrations were filtered to measure the concentration of free adenylosuccinate. The dissociation constant was determined from the Scatchard equation, $r/[L] = (-1/K_d)r + n/K_d$, where K_d is the dissociation constant, [L] is the concentration of the free adenylosuccinate, n is the number of binding sites, and r is $[EL]/[E]_0$ is the ratio of the concentration of enzyme−substrate complex to the total enzyme concentration. K_d is equal to (−1/slope) from the plot of *r*/[L] against *r*. A representative plot for H141E is shown in Figure 4.

Table 2 summarizes the results of these adenylosuccinate-binding measurements. Note that this method cannot be used to assess the dissociation constant for the complex of adenylosuccinate and wild-type enzyme; this active enzyme would rapidly catalyze the cleavage of adenylosuccinate before measurements could be made. Instead, the K_d for adenylosuccinate−wild-type enzyme complex was estimated from the ability of adenylosuccinate to inhibit the reverse reaction of AMP + fumarate. Adenylosuccinate was found

Table 2: Dissociation Constants of Adenylosuccinate by Mutant Enzymes

	K_d (μM)
H141A	180
H141L	196
H141E	42
H141Q	71
H68A	52
H68K	69

to be a competitive inhibitor with respect to AMP with a K_I value of 4.6 μM. As shown in Table 2, the constants for mutant enzymes are about 10−40-fold higher than that for the wild-type, indicating that these mutations have greater effects on substrate binding than do the H141R and H68Q mutations. Nevertheless, all of the mutant enzymes retain the ability to bind adenylosuccinate, albeit with weaker affinity.

pH Dependence of Reaction Catalyzed by Adenylosuccinate Lyase. The kinetic studies at different pHs were carried out to evaluate the effects on the ionizable groups caused by the mutations. Analyses were performed on the H68Q, R67M, H141R, R67M:H68Q, and wild-type enzymes. (Other mutant enzymes were too inactive to measure.) Detailed studies on k_{cat} and K_m for all enzymes show that the K_m for adenylosuccinate is little changed over the pH range from 6 to 9. On the basis of this observation, we made the assumption that the mutations do not alter pH independence of the affinity of enzyme for substrate; thus, both k_{cat}/K_m vs pH and V_{max} vs pH would render ionizable groups with same pK_a values. Measurements were thus made at the single, relatively high substrate concentration (100 μM adenylosuccinate) in order to generate the pH profile.

Bell-shaped curves were observed for all enzymes investigated over the pH range 6−9. The data were fitted to the following equation by nonlinear regression:

$$V = \frac{V_o}{1 + 10^{(pK_1 - pH)} + 10^{(pH - pK_2)}} \quad (4)$$

where V is the measured activity at certain pH; V_o represents the intrinsic value of V (pH independent); and pK_1 and pK_2 are the pK_a values for the two ionizable groups responsible for the left limb and right limb, respectively. The data were analyzed using GraphPad software InPlot for least-squares parameter evaluation, where the V_o and the two pK_a values were determined. To compare the effects on the pK_a values caused by mutations, each set of data was normalized to $1/f^-$ by its own V_o according to the following equation,

$$\frac{1}{f^-} = \frac{V}{V_o} = \frac{1}{1 + 10^{(pK_1 - pH)} + 10^{(pH - pK_2)}} \quad (5)$$

where f^- is the Michaelis pH function for the active form of the enzyme (*26*). Figure 5 superimposes the plots of $1/f^-$ against pH. Since the $1/f^-$ is independent of intrinsic specific activity, it reflects solely the effects on pK_1 and pK_2. The pK_a values for each enzyme are summarized in Table 3. The H141R mutation increases pK_1 by 0.8 unit without affecting pK_2, whereas the R67M mutation mainly increases pK_2. The H68Q and R67M/H68Q mutations have little effect on the pH profile.

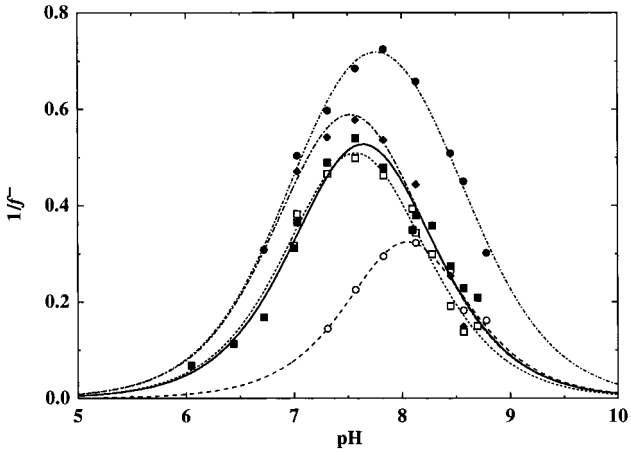

FIGURE 5: pH profiles for the wild-type and mutant enzymes. The activities in different pH buffers were measured for the wild-type (■), H141R (○), H68Q (□), R67M (●), R67M:H68Q (◆) as described in Experimental Procedures. The data were normalized to $1/f^-$ for comparison (see text).

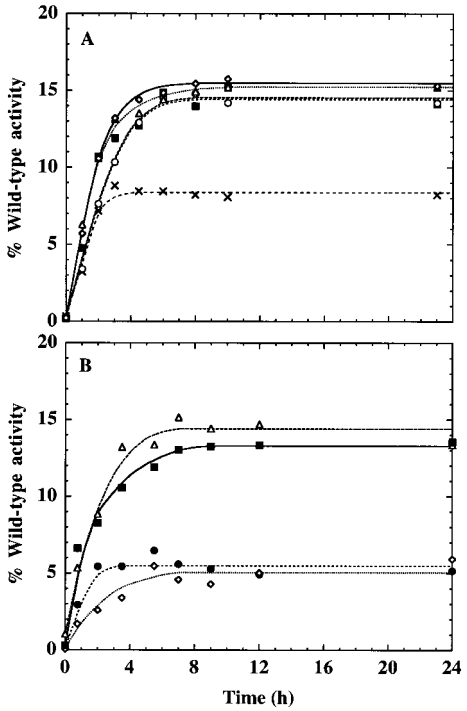

FIGURE 6: Time-dependent reactivation of mixture of His[141] and His[68] mutants. The mixtures of two mutants were incubated in 20 mM potassium phosphate (pH 7.0) containing 20 mM NaCl at 25 °C. (A) Mixtures between H68Q and H141A (◇), H141L (△), H141E (○), H141Q (■), and H141R (×). (B) Mixtures between H141Q and H68Q (■), H68A (◇), H68K (●), and R67M:H68Q (△). The final concentration of each mutant in the incubation mixture was 0.7 mg/mL. The activities of the hybrids were compared with that of the wild-type enzyme (1.4 mg/mL) incubated under the same conditions to calculate the percentage of wild-type activity.

Intersubunit Complementation by His[141] and His[68] Mutants. Many multimeric proteins exhibit intersubunit complementation behavior, in which two inactive enzymes with mutations at distinct positions can each contribute a subunit with a wild-type amino acid at a different position to constitute an active site. Such complementation, with the restoration of activity in hybrids of two distinct inactive mutant enzymes, provides strong evidence for the existence of intersubunit functional sites. The combination of inactive His[141] and His[68]

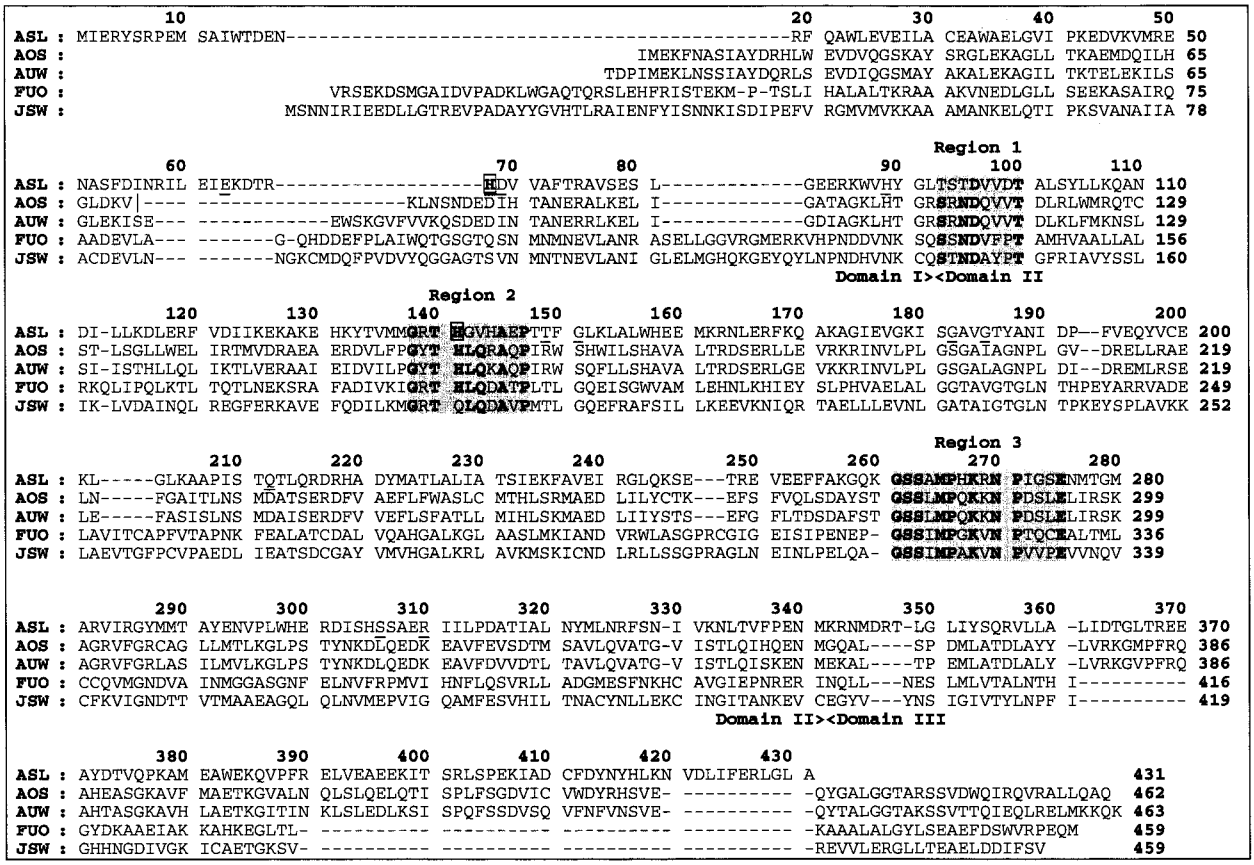

FIGURE 7: Amino acid sequence alignment of adenylosuccinate lyase (ASL), human argininosuccinate lyase (AOS), duck δ2-crystallin (AUW), *E. coli* fumarase (FUO), and *E. coli* aspartase (JSW). The alignment was subjected to Modeler for model building. The sequences of the reference proteins were extracted from their structures. The vertical bar (|) in AOS (after V70) indicates a segment of nine missed residues in the coordinates. The dash (−) stands for a gap. The sequence number of ASL is labeled on the top and those of the rest are on right of the alignment. Domains **I** (1−92), **II** (93−341), and **III** (342−431) are also marked below the sequences. The three highly conserved regions are highlighted with dark background, with those conserved residues in bold. The 21 residues completely conserved in all 15 adenylosuccinate lyases are underlined. The His[68] and His[141] are boxed.

Table 3: pK_a Values Determined by Fitting Data from Figure 5 to eq 5

	pK_1	pK_2
wild-type	7.3	8.0
H141R	8.1	8.0
H68Q	7.3	7.9
R67M	7.1	8.5
R67M:H68Q	7.1	8.0

mutant adenylosuccinate lyases demonstrates complementation.

Incubation of mixtures containing a His[141] mutant with a His[68] mutant in 20 mM potassium phosphate (pH 7.0) containing 20 mM NaCl at 25 °C results in the dramatic appearance of the enzymatic activity (Figure 6). The reactivation process is maximal within about 4 h. Each mutant was mixed with a glutamine mutant for the other histidine. All combinations of His[141] and His[68] mutants yielded marked activation and reached 5−15% of the wild-type activity. Therefore, the reactivation is not due to combinations of specific mutations, but is a result of subunit complementation. Table 4 reports the K_m values and the relative activities of each pair of hybrid enzymes. The K_m values are within 7-fold of that of the wild-type. The differences may be caused by the minor perturbation of the structure by mutations. These results strongly suggest that the adenylosuccinate lyase acts as a multimer and that His[141] and His[68] come from different subunits to form the active site.

Table 4: Relative Activity and K_m Values of the Reconstituted Hybrid Adenylosuccinate Lyase[a]

	relative activity	K_m (μM)
wild-type	1.00	2.6 ± 0.4
H141A + H68Q	0.15	6.3 ± 1.3
H141L + H68Q	0.15	5.5 ± 0.8
H141E + H68Q	0.14	7.9 ± 1.2
H141Q + H68Q	0.15	8.4 ± 1.2
H141R + H68Q	0.08	13.3 ± 3.7
H141Q + H68Q	0.13	9.2 ± 1.8
H141Q + H68A	0.05	17.5 ± 1.6
H141Q + H68K	0.05	10.1 ± 1.3
H141Q + R67M:H68Q	0.14	12.3 ± 2.7

[a] The specific activities were measured under standard assay conditions, as described in the Experimental Procedures. The K_m constants were determined by varying the concentration of adenylosuccinate and fitting the data into the Michaelis−Menten equation.

DISCUSSION

Characterization of the site-directed mutant forms of *B. subtilis* adenylosuccinate lyase with replacements for His[141] clearly demonstrates the importance of this residue. Five amino acid substitutions were chosen to examine the function of His[141]. Alanine and leucine are two hydrophobic residues of different sizes. Glutamic acid and arginine are, respec-

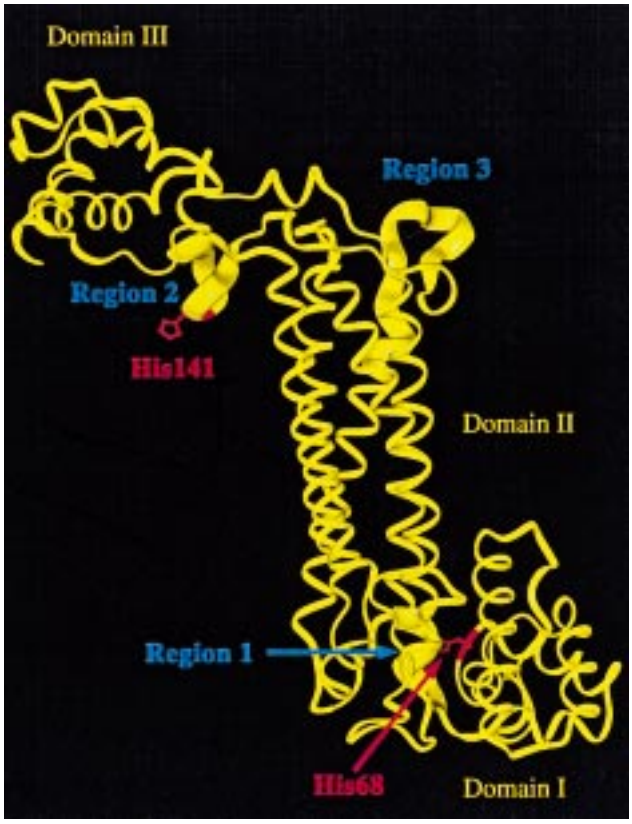

FIGURE 8: Ribbon diagram of the model structure of subunit A of adenylosuccinate lyase. Domain **I**, **II**, and **III** are located, respectively, at the bottom right, middle and top left of the drawing. The three conserved regions are drawn with wider ribbons. The two histidines are colored in red.

tively, negatively and positively charged. Glutamine is similar in size, hydrophobicity and hydrogen-bonding ability to histidine, but lacks the ability to act as a general base−general acid catalyst. Except for H141R, all mutations abolished catalytic activity. Even for H141R, the activity is reduced by 10^5-fold. In *E. coli* fumarase C, the mutant of the corresponding histidine H188N is ~200 times less active than wild-type (*24*). Such a mutation in duck δ-crystallin (H162N) causes complete loss of activity (*27*). The mutant enzymes are so inactive that it is virtually meaningless to distinguish on the basis of their activities between the different effects caused by the mutations. The large decrease in k_{cat} and relatively small increase in K_m observed in H141R suggests that His^{141} is involved in catalysis rather than substrate binding. These results are similar to those we reported for His^{68} mutants (*13*) and are consistent with our previously proposed role for His^{141} as a general base catalyst (*12*).

Circular dichroism spectroscopy and gel filtration chromatography were conducted on all His^{141} and His^{68} mutants to evaluate whether the loss of activity is caused by significant structural alteration or dissociation of the tetramer. The results (Figures 2 and 3) indicate that the mutations have little effect on these properties. Therefore, the functions of these two residues are not likely related to tetramer formation or to overall enzyme conformation.

The binding constants of radioactive adenylosuccinate were determined for the inactive mutants. Compared with the K_I for the wild-type enzyme, the mutants exhibit 10−40 times weaker affinity for substrate. This factor could contribute to the negligible activities of these mutants, while H141R and H68Q are partially active. However, the effects on affinity alone cannot account for the total loss of activity, as the detection level is at least 10000-fold below the wild-type activity. Therefore, these results are consistent with our hypotheses for the catalytic roles of these two histidines.

Since both His^{141} and His^{68} are essential for catalysis and both of them are absolutely conserved in 15 sequences of adenylosuccinate lyase, it is natural to assign the general acid−base pair to these two histidines. Our results from pH-dependent studies not only support this hypothesis, but also provide insight to differentiate the functions of the two.

The pK_1 and pK_2 of the wild-type are 7.3 and 8.0. These values are somewhat higher than 6.4 and 7.5 reported for the recombinant human enzyme (*7*), and 6.4 and 8.2 reported for the rat muscle enzyme (*8*). The H141R mutation markedly increases the pK_1 value (by 0.8 unit) without changing pK_2, indicating that His^{141} is responsible for the pK_1 of 7.3 in the wild-type enzyme. If pK_1 represents an amino acid residue other than His^{141}, the only way the H141R mutation could change its value is by changing the environment around this residue. The mutation could either introduce a positive charge to the site (provided His^{141} is unprotonated in the wild-type) or maintain the positive charge (provided His^{141} is protonated in the wild-type). The former would be expected to decrease pK_1 instead because the additional positive charge would strengthen the acidity of the proximal ionizable group. The latter would keep the pK_1 unchanged. Since neither of these effects were observed, this scenario is not likely to be correct. Rather, the pK_1 of 7.3 in the wild-type enzyme probably represents His^{141}. The pK_1 of 8.1 observed in H141R is likely contributed by another residue in the site revealed in the absence of His^{141}. This result is consistent with the hypothesis that His^{141} is the general base in the catalytic reaction.

In contrast, very little change in the pH dependence was observed in H68Q. The R67M mutation increases pK_2 by 0.5 unit, indicating the removal of the positive charge of arginine increases pK_a of the ionizable group; Arg^{67} may therefore be close to the protonated group represented by pK_2, possibly His^{68}. However, this effect disappears in the R67M:H68Q double mutant. It is possible that another ionizable amino acid, distant from Arg^{67}, substitutes for His^{68} as the general acid in the H68Q and double mutant.

Molecular modeling was performed to gain more structural insight into our experimental results. The model of ASL was constructed using four reference structures in the fumarase superfamily. Because of the low homology across the family, we took advantage of Modeler for its ability to simultaneously incorporate structural data from more than one reference protein. Since the most critical step of modeling is the sequence alignment, it was most extensively and carefully studied. The methods employed include both sequence and structural alignment. The optimum alignment was obtained by integration of the pairwise alignment and refined later by the molecular PDF violations calculated by Modeler.

Figure 7 reports the final multiple alignment which was used for the model generation. Note that there are no completely conserved residues outside the three conserved regions and all three conserved regions reside in domain **II**, making it the most conserved domain of the three. It should

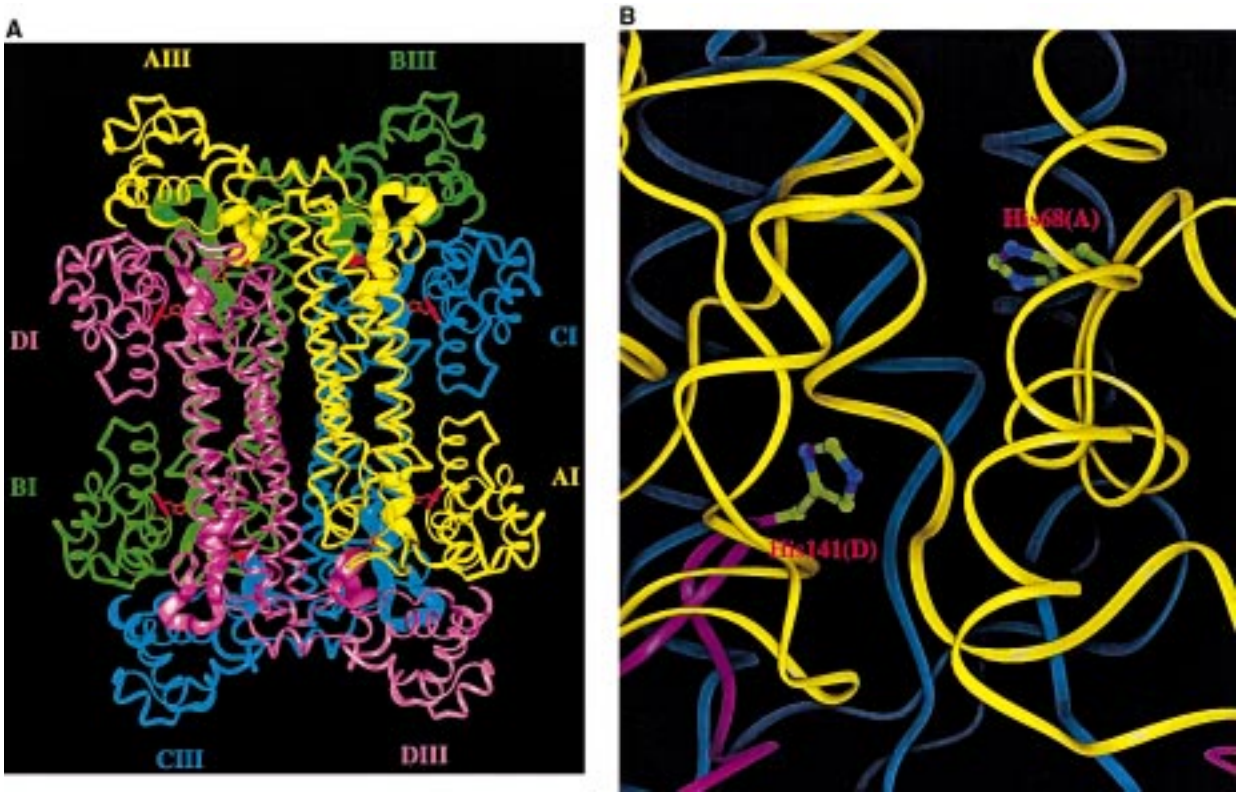

FIGURE 9: The subunit association of adenylosuccinate lyase. (A) The ribbon structure of the tetrameric form of adenylosuccinate lyase. The four subunits are displayed in their Cα backbone trace. Domains **I** and **III** of each subunit are labeled at the outside of the structure. The color code for subunits is A, yellow; B, green; C, blue; and D, pink. The three conserved regions and the two histidines are drawn in the same way as shown in Figure 8 for the A subunit. (B) Enlargement of the active site at the bottom-right corner of the tetramer, including the **DIII**-**AI** domains. The active sites are formed by residues from three subunits. The side chains of His^{141} (from subunit D) and His^{68} (from subunit A) are shown in ball-and-stick colored by atoms: C, green; N, blue.

also be pointed out that there are four segments in adenylosuccinate lyase which are not aligned with any reference protein sequence. That does not necessarily mean that, in the actual structure, these residues share no structural homology with the reference proteins; rather, Modeler does not use such homology, if it exists. The program thus randomly generates loops for these segments. These regions include the residues 1−18, 58−67, 346−348, and 420−431.

As outlined in the Experimental Procedures, the model of the ASL monomer was generated by using the High optimization protocol, and among five models which were compared, the one with the lowest *F* value was selected as the best model. Figure 8 shows the model of the adenylosuccinate lyase monomer. Like the reference proteins, the adenylosuccinate lyase monomer contains three structural domains which can easily be distinguished. Domain **I** and domain **III** form the two lobes at each end of the dumbbell-like structure. Domain **II** contains five long α-helices connecting domain **I** and domain **III**. As shown in Figure 8, the three highly conserved regions (shown with wider ribbons) are well separated in space, making it impossible that they participate in a single active site. It must be the tetrameric structure that brings them together. Also shown in Figure 8 are His^{141} and His^{68}, which are separated by the long helices. His^{141} belongs to the conserved region 2 and is at the conjunction of domains **II** and **III**, projecting out of the loop. His^{68} is in domain **I** and not in one of the regions conserved in all members of the superfamily, although it is spatially close to the conserved region 1 and it is found in adenylosuccinate lyases from all 15 species examined.

The tetrameric adenylosuccinate lyase molecule was generated by subunit assembly and energy minimization. The structure of the tetramer is illustrated in Figure 9A. The association of the monomers mainly involves hydrophobic interactions through domain 2 of each subunit. Subunit A has a head-to-head arrangement with subunit B and a head-to-tail arrangement with subunit D. The 20 α-helices form a bundle tethering the tetramer, while the active sites locate at the four corners of the structure.

An enlargement of one active site is shown in Figure 9B. The active site is surrounded by the three conserved regions from different subunits which form a big pocket (Figure 9B). The two histidine residues in an active site are pointing to each other. Note the pairing of the two histidines, i.e., the histidines from subunit A pair with that from subunit D, whereas the histidines from subunit B pair with those from subunit C. This observation provides the molecular basis for the subunit complementation.

From the structure of the tetramer, it is clear that each subunit provides His^{141} and His^{68} to two active sites, and each active site contains the two histidines from different subunits. The existence of this intersubunit active site is strongly supported by the complementation experiments. Moreover, intragenic complementation has been reported for argininosuccinate lyase (*14*, *28*), another tetrameric enzyme in the superfamily. A noteworthy observation is the reported complementation between D87G and Q286R mutants of argininosuccinate lyase (*29*). Sequence comparison indicates that His^{68} of adenylosuccinate lyase aligns with Asp^{87} of argininosuccinate lyase, and His^{141} of adenylosuccinate lyase

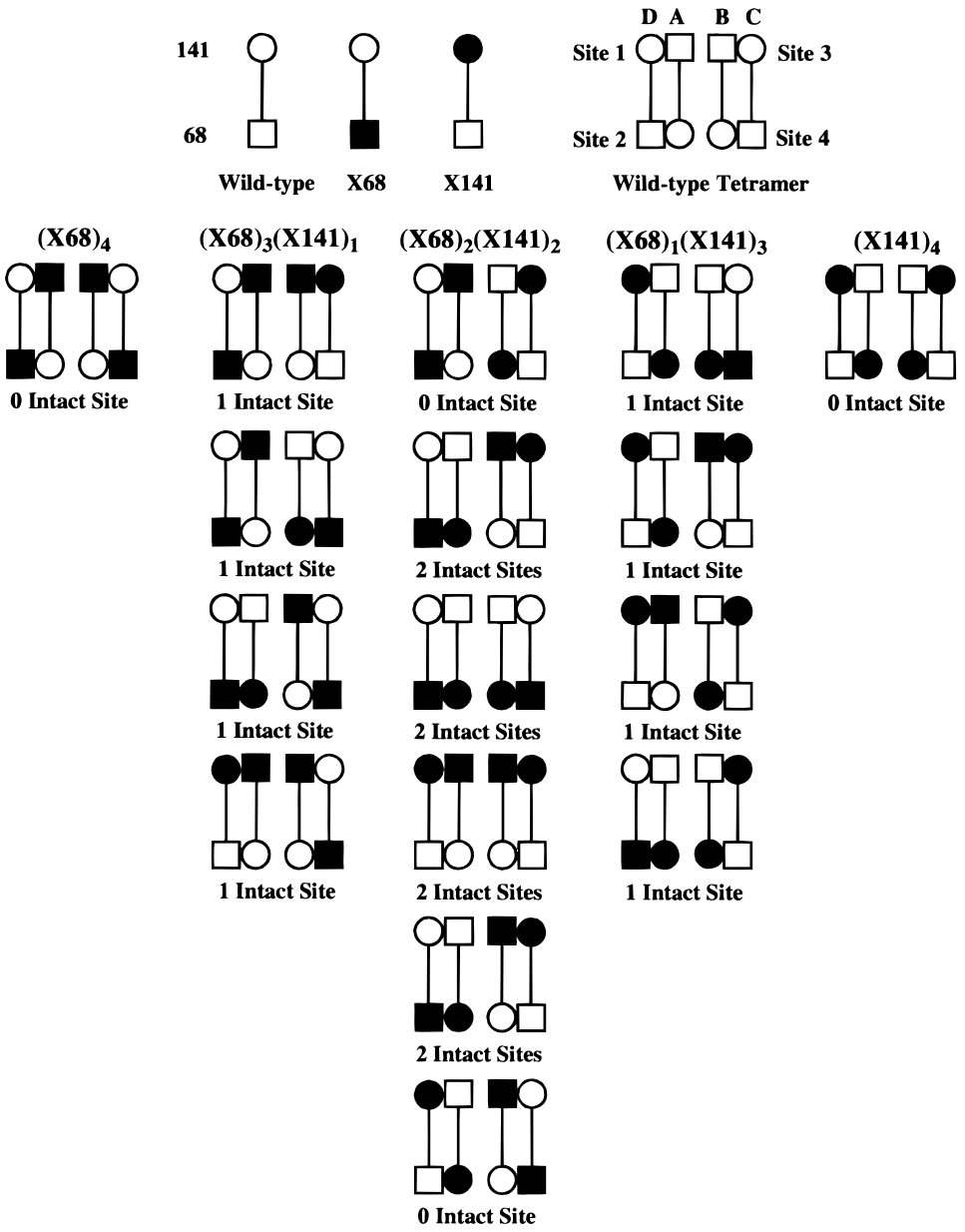

FIGURE 10: Schematic representation of reconstitution of active sites by intersubunit complementation. His^{68}, His^{141}, mutant residue for His^{68}, and mutant residue for His^{141} are represented by □, ○, ■, and ●, respectively. Wild-type subunit, His^{68} mutant subunit (X68), and His^{141} mutant subunit (X141) are represented by □—○, ■—○, and □—●, respectively. □○ stands for the intact active sites, whereas ■○, □●, and ■● stand for the damaged active sites. The alignment of subunits in a tetramer is D → A → B → C from left to right. The strong interactions of AD and BC are shown. The five combinations of the two mutant subunits generate 16 distinct arrangements. Sixteen of the overall 64 active sites are intact.

is equivalent to His^{160} of argininosuccinate lyase (Figure 7). In the structure of human argininosuccinate lyase, the active site contains Asp^{87} and His^{160} from different subunits (*14*).

Recovery of adenylosuccinate lyase activity was observed in the present study during incubation of each pair of inactive His^{141} and His^{68} mutants. There must be an equilibrium in the solution between the tetramer and dimer and/or monomer (even though our gel filtration experiments indicate that the tetramer is the predominant species). The dissociation and reassociation scrambles the two types of mutant subunits leading to hybrid enzyme with recovered active sites. Figure 10 illustrates every possible hybridization and theoretical number of "intact" active sites generated by random recombination of His^{141} mutant subunits and His^{68} mutant subunits. There are five possible combinations in terms of ratio of the two mutants in the tetramer, i.e., 4:0, 3:1, 2:2, 1:3, and 0:4, as shown by the columns. The number of possible permutations for each combination can be calculated by C_4^n, where n is the number of either mutant subunit in the tetramer. This gives 1, 4, 6, 4, and 1 possibilities, respectively. As illustrated in Figure 10, 16 out of 64 active sites are intact active sites (□○). Therefore, the expected apparent activity is 25% that of wild-type enzyme.

The observed activities of 5−15% are significantly higher than the individual mutants, but lower than expected. One possible explanation for this observation is that the scrambling of mutant subunits is not totally random. Inspection of the interaction between subunits in the model structure (Figure 9A) indicates that there are three types of subunit interface in the tetramer judged by the hydrophobic interaction between α-helices in domain 2: the strongest interac-

tions (AD and BC), the weaker interactions (AC and BD), and the weakest interactions (AB and CD). The strong association between A and D (or B and C) probably makes them difficult to separate under the conditions of incubation, resulting in incomplete randomization. This proposed pattern of subunit interaction is a common feature throughout the superfamily. Both bovine argininosuccinate lyase and chick δ-crystallin can dissociate into dimers at 4 °C, but cannot be separated into monomers without denaturation (*30*, *31*). Our attempts at denaturation followed by renaturation did not provide reactivation. The conditions employed (e.g., urea or cetyltrimethylammonium bromide) may have been too harsh to allow refolding of the protein.

The active-site cleft is clearly visible in Figure 9. The distance between ϵ-N of His^{141}(D) and ϵ-N of His^{68}(A) is 8.56 Å, and the distances from N-3 to the β carbon and terminal carboxyl carbon of adenylosuccinate in the anti-configuration are 6.57 and 7.70 Å, respectively: the substrate can clearly be accommodated in the region between the two histidines. In the active site of *E. coli* fumarase C-inhibitor complexes, the C-1 carboxylate of citrate was found to interact with Lys^{324} and Asn^{326}. The C-3 carboxylate interacts with Ser^{140} (*19*). These residues also interact with carboxylates of pyromellitic acid (*19*). Likewise, in the active site of yeast fumarase cocrystallized with meso-tartrate, one carboxylate interacts with Lys^{349} and Asn^{351}, while the other interacts with Ser^{165} (*25*). The equivalent residues in *B. subtilis* adenylosuccinate lyase, Lys^{268}, Asn^{270}, and Ser^{94} are in conserved regions 1 and 3 of the family and are completely conserved in adenylosuccinate lyase (Figure 7). On the basis of these analogies, we were able to dock a molecule of adenylosuccinate into the active site formed by subunits A, C, and D (Figure 9B). The substrate could be positioned so that the two carboxylates of the succinyl moiety were close to the above three residues, after energy minimization. However, more than one orientation of adenylosuccinate results in similar energy states for the enzyme−substrate complex. The molecular model we have constructed provides the basis for testable hypotheses about the active site. However, a more detailed description of the active site must await experimental evaluation by further mutagenesis and structural studies.

The results of this study clearly demonstrate that the active site of adenylosuccinate lyase contains His^{141} and His^{68} from two different subunits. While both of these amino acid residues are important in catalysis, His^{141} is likely to serve as the general base catalyst, and His^{68} as the general acid.

REFERENCES

1. Ratner, S. (1972) in *The Enzymes* (Boyer, P. D., Ed.) Vol. 7, 3rd ed., pp 167−197, Academic Press, New York.
2. Jaeken, J., and Van den Berghe, G. (1984) *Lancet 2*, 1058−1061.
3. Van den Berghe, G., Bontemps, F., Vincent, M. F., and Van den Bergh, F. (1992) *Prog. Neurobiol. 39*, 547−561.
4. Van den Berghe, G., Van den Berghe, F., Francoise, V., and Jaeken, J. (1995) in *Purine and Pyrimidine Metabolism in Man VIII* (Sahota, A., and Taylor, M., Eds.) pp 363−366, Plenum Press, New York.
5. Verginelli, D., Luckow, B., Crifo, C., Salerno, C., and Gross, M. (1998) *Biochim. Biophys. Acta 1406*, 81−84.
6. Maaswinkel-Mooij, P. D., Laan, L. A., Onkenhout, W., Brouwer, O. F., Jaeken, J., and Poorthuis, B. J. (1997) *J. Inherit. Metab. Dis. 20*, 606−607.
7. Stone, R. L., Zalkin, H., and Dixon, J. E. (1993) *J. Biol. Chem. 268*, 19710−19716.
8. Casey, P. J., and Lowenstein, J. M. (1987) *Biochem. J. 246*, 263−269.
9. Bridger, W. A., and Cohen, L. H. (1968) *J. Biol. Chem. 243*, 644−650.
10. Bridger, W. A., and Cohen, L. H. (1969) *Can. J. Biochem. 47*, 665−672.
11. Hanson, K. R., and Havir, E. A. (1972) in *The Enzymes* (Boyer, P. D., Ed.) Vol. 7, 3rd ed., pp 75−166, Academic Press, New York.
12. Lee, T. T., Worby, C., Dixon, J. E., and Colman, R. F. (1997) *J. Biol. Chem. 272*, 458−465.
13. Lee, T. T., Worby, C., Bao, Z.-Q., Dixon, J. E., and Colman, R. F. (1998) *Biochemistry 37*, 8481−8489.
14. Turner, M. A., Simpson, A., McInnes, R. R., and Howell, P. L. (1997) *Proc. Natl. Acad. Sci. U.S.A. 94*, 9063−9068.
15. Li, Y., Feng, L., and Kirsch, J. F. (1997) *Biochemistry 36*, 15477−15488.
16. Kang, C., Kim, S., and Fromm, H. J. (1996) *J. Biol. Chem. 271*, 29722−29728.
17. Goyal, A., Aghajanian, S., Hayden, B. M., Wang, X. G., and Engel, P. C. (1997) *Biochemistry 36*, 15000−15005.
18. Redinbo, M. R., Eide, S. M., Stone, R. L., Dixon, J. E., and Yeates, T. O. (1996) *Protein Sci. 5*, 786−788.
19. Weaver, T., and Banaszak, L. (1996) *Biochemistry 35*, 13955−13965.
20. Shi, W., Dunbar, J., Jayasekera, M. M., Viola, R. E., and Farber, G. K. (1997) *Biochemistry 36*, 9136−9144.
21. Abu-Abed, M., Turner, M. A., Vallee, F., Simpson, A., Slingsby, C., and Howell, P. L. (1997) *Biochemistry 36*, 14012−14022.
22. Altschul, S. F., Madden, T. L., Schaffer, A. A., Zhang, J., Zhang, Z., Miller, W., and Lipman, D. J. (1997) *Nucleic Acids Res. 25*, 3389−3402.
23. Huang, X., and Miller, W. (1991) *Adv. Appl. Math. 12*, 337−357.
24. Weaver, T., Lees, M., and Banaszak, L. (1997) *Protein Sci. 6*, 834−842.
25. Weaver, T., Lees, M., Zaitsev, V., Zaitseva, I., Duke, E., Lindley, P., McSweeny, S., Svensson, A., Keruchenko, J., Keruchenko, I., Gladilin, K., and Banaszak, L. (1998) *J. Mol. Biol. 280*, 431−442.
26. Dixon, M., and Webb, E. C. (1964) in *Enzymes*, 2nd ed., pp 116−145, Academic Press, New York.
27. Patejunas, G., Barbosa, P., Lacombe, M., and O'Brien, W. E. (1995) *Exp. Eye. Res. 61*, 151−154.
28. McInnes, R. R., Shih, V., and Chilton, S. (1984) *Proc. Natl. Acad. Sci. U.S.A. 81*, 4480−4484.
29. Walker, D. C., Christodoulou, J., Craig, H. J., Simard, L. R., Ploder, L., Howell, P. L., and McInnes, R. R. (1997) *J. Biol. Chem. 272*, 6777−6783.
30. Lusty, C. J., and Ratner, S. (1972) *J. Biol. Chem. 247*, 7010−7022.
31. Piatigorsky, J., Horwitz, J., and Simpson, R. T. (1977) *Biochim. Biophys. Acta 490*, 279−289.

BI982299S